IL NUOVO CIMENTO Vol. 36 C, N. 2 Marzo-Aprile 2013
DOI 10.1393/ncc/i2013-11512-8

Colloquia: Nanoforum 2012

Tunable plasmon resonance nanostructures: SERS application in wines identification

A. Serra([1]) and D. Manno([2])

([1]) *Phyisics Applied to Materials Science PAMS Laboratory Dep. BBCC University of Salento Lecce, Italy*
([2]) *Phyisics Applied to Materials Science PAMS Laboratory DISTeBA University of Salento Lecce, Italy*

ricevuto il 25 Febbraio 2013

Summary. — A real-time and sensitive methodology has been developed and optimized to detect water-soluble molecules by surface-enhanced Raman spectroscopy (SERS). Silver nanoparticles were synthesized by using erytrithol and fructose as capping and reducing agents, respectively. The proposed method can be successfully applied to solve problems and obtain optimal Raman spectra also from organic dyes or specific phenolic compounds highly fluorescent. In this work we illustrate the potentiality of the methodology applying it to the characterization of red wine, which, as we know, it is very difficult to be analyzed by Raman spectroscopy precisely because of the strong fluorescence of the phenolic compounds that give red wine its typical and popular features.

PACS 78.67.Bf – Nanocrystals, nanoparticles, and nanoclusters.
PACS 68.37.-d – Microscopy of surfaces, interfaces, and thin films.
PACS 42.79.Pw – Imaging detectors and sensors.

1. – Introduction

Plasmonic nanoparticles, typically silver or gold, offer much potential for novel optical sensor device development. Their interesting plasmonic properties are based on the collective oscillation of their conductive electrons. This oscillation results in a strong plasmon band, known as localized surface plasmon resonance (LSPR). LSPR spectral position and properties (*i.e.* extinction) can be adjusted by varying the material, particle size, and shape of chemically synthesized colloidal particles [1]. Plasmonic nanoparticles are extremely sensitive to their local environment, *e.g.* analyte binding to the nanoparticles. The local changes in the refractive index induce a shift in the LSPR peak position [2]. Sensors for detecting this change can use nanoparticles in an ensemble, such as in solution or monolayers, but also at the single particle level and were exploited for wide-ranging applications, from biological and chemical sensors based on changes in

near-surface refractive index or Raman scattering [3], Bragg reflection [4], photo detection [5], lasers and solar-energy generation [6]. Methods to modify plasmonic interactions by controlling the shapes and sizes of the metal structures [7], the types of metals [8] or the indices of refraction of the surrounding materials [9] are firmly established. Newer approaches integrate plasmonic components into equivalent circuit structures such as metalinsulatormetal stacks [10].

Furthermore, a local field enhancement is observed, which is the basis for applying plasmonic nanoparticles for surface enhanced Raman spectroscopic (SERS) techniques [11]. The theory of SERS is now largely established, is a phenomenon in which the Raman scattering intensity from molecules close to the surface of certain finely divided metals is enhanced by a factor of about 10^6. The sequence of events leading to the first observation of SERS were described in a recent note by McQuillan [12]. Most of the enhancement arises from the concentration of the electromagnetic optical fields near appropriately designed gold or silver nanosystems that are excited at or near surface-plasmon resonances [13] and provide molecular fingerprint information that is particularly valuable in chemistry. The vibrational information allows molecular species to be detected and identified [14, 15]. The SERS enhancement can be so great that analytes with femtomolar or lower concentrations can be detected [16]. The idea to develop the synthesis of colloidal solutions containing silver or gold nanostructures, capable of binding to themselves the molecular species to be detected, and thus obtain SERS effect in the fluid, can be decisive for a lot of applications. This paper provides a useful perspective to examine analytes of different nature beyond the current limits and assess possible future directions of SERS as a bioanalytical tool. In this work, we solved the problem of fluorescence using the SERS-induced by silver nanoparticles with a plasmons in tune with the wavelength of the laser used. In this way we obtained the enhanced Raman spectrum coming from molecules present in a wine. We developed this method and demonstrated its applicability in the case of different origin guarantied Italian (DOC) red wines. The SERS provided a substantial spectral enhancement and therefore good quality spectra of red wine samples and the obtained spectra reveal the characteristics of the wines highlighting the compositional differences that determine the organoleptic features. The SERS profile allows the determination of the fingerprints of samples and indisputable recognition of the particular wine. This technique represents a valuable method by which the sophistication of quality wines can be countered.

2. – Experimental

2˙1. *Chemicals.* – Silver nitrate ($AgNO_3$, 99%) fructose ($C_6H_{12}O_6$, 99%) and erythritol ($C_4H_{10}O_4$, 99%) were from Sigma-Aldrich and used as received. Deionized ultra-filtered water prepared with a Milli-Q water purification system was used throughout. In a typical preparation, 0.15 M aqueous fructose and 0.15 M aqueous erythritol were dissolved in 200 ml of deionized water. Then a 2 ml aliquot of a 10^{-2} M aqueous solution of $AgNO_3$ was added. This reaction mixture was exposed to high intense microwave irradiation (800W) in a domestic microwave oven operating in a cycling mode (on 5 s, off 10 s) to prevent boiling of solvent [17]. The colour of the reaction solution became pale yellow after 4 min indicating the formation of silver nanoparticles.

2˙2. *UV-Vis analysis.* – UV-visible spectra were recorded in the range between 300 and 800 nm using a Varian Cary-5 spectrophotometer. Solution spectra were obtained by measuring the absorption of the prepared nanoparticle dispersions in a quartz cuvette

TABLE I. – *Wine details.*

Denomination	Wine type grapes	Origin
Lambrusco	100% Lambrusco Sorbara	San Lorenzo (Modena)
Brunello di Montalcino	100% Sangiovese	Montalcino (Siena)
Nero d'Avola	100% Nero d'Avola	Noto (Siracusa)
Primitivo	100% Primitivo	Manduria (Taranto)
Rosato	90% Negramaro 10% Malvasia	Salice Salentino (Lecce)

with a 1 cm optical path. In addition, to evaluate the successful interaction between the molecular species of wine and nanoparticles, UV-VIS spectra were obtained by mixing a colloidal solution and wine. In both cases the experimental data were corrected for the background absorption of the solution.

2˙3. *TEM observations.* – The morphology of the Ag-NP, before and after having interacted with the wine, was carefully investigated using a transmission electron Hitachi H-7100 microscope operated at an accelerating voltage of 100 kV. The TEM samples were prepared by placing small drops of colloidal solutions of Ag-NP, and even of colloidal solutions of Ag-NP after the interaction with the wine, onto standard carbon supported 600-mesh copper grid and drying slowly in air naturally. All the measurements were carried out at room temperature.

2˙4. *Raman spectroscopy.* – The Raman spectra were recorded with a Renishaw InVia spectrometer equipped with a Leica optical microscope. The excitation source was the 514.5 nm output of an Ar^+-ions laser working at a maximum output power of 25 mW. All spectra were recorded using a resolution of 1.5 cm^{-1} over the spectral range 150–3000 cm^{-1}. All spectra were recorded at room temperature. For the Raman measurements, the wine samples were taken out from the refrigerator and returned to 22 °C. The wine sample (50 μl) was mixed with 10 μl Ag colloid and placed in a quartz cuvette (QG, Hellma, NY, USA) to reduce the interfering fluorescence signals that occur with glass or plastic cuvettes, during the spectrum acquisition. The Raman spectra were acquired for 20 seconds and a relatively good signal-to-noise ratio was obtained from the samples.

2˙5. *Wine samples.* – In this experiment we analyzed some DOC Italian red wines from local market, described in table I. The analyzed wines were from the 2010 vintage, harvested in different regions of Italy and collected from bottles after the completion of the malolactic fermentation. The *p*H values of these wines were of about 3.7 for all the samples.

3. – Results and discussion

3˙1. *UV-Vis and TEM analysis.* – The UV-Vis spectrum recorded from the obtained colloidal solution is shown in fig. 1a. A typical transmission electron microscope image of the synthesized silver nanoparticles is shown in fig. 1b. One can see well-dispersed spherical Ag nanoparticles, with a size ranging from 1.5 to 25 nm. The inset of fig. 1b shows a nanoparticle surrounded by a corona having 2 nm in thickness. To determine the nanoparticles size distribution a lot of digitalized HREM images, performed onto 50 randomly chosen fields, were processed by Image Pro-Plus software and the obtained

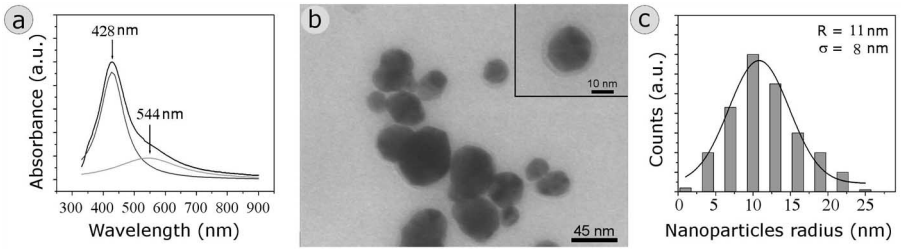

Fig. 1. – UV-Vis spectrum (a); transmission electron microscope image (b); nanoparticles size distribution (c) recorded from Ag colloidal solution.

data were reported in the histogram of fig. 1c. The monodisperse size distribution was fitted by a Gaussian curve that allow to determine nanoparticles average size $d = 11.0\,\text{nm}$ and standard deviation $\sigma = 8.0\,\text{nm}$.

After interaction of the colloidal solution with the wine we obtain a modification of the UV-Vis spectrum as well as the morphological features of Ag nanoparticles. As an example in fig. 2a we report the UV-Vis spectrum recorded from the mixture colloidal solution-primitivo wine. A typical transmission electron microscope image of this mixture is shown in fig. 2b.

One can spherical Ag nanoparticles, with a radius ranging from 1.5 to 35 nm. The nanoparticle surrounded by a corona having about 8 nm in thickness. To determine the nanoparticles size distribution, also in this case, a lot of digitalized HREM images were processed and the obtained data were reported in the histogram of fig. 1c. The polidispersed size distribution was fitted by two Gaussian curves that allow to determine two groups of nanoparticles the first has average size $d = 5.0\,\text{nm}$ and standard deviation $\sigma = 2.0\,\text{nm}$, and the second one has average size $d = 22.0\,\text{nm}$ and standard deviation $\sigma = 9.0\,\text{nm}$. The UV-Vis spectrum of the colloidal solution (fig. 1a) shows a pronounced peak of plasmon resonance at 428 nm and a less evident at 544 nm. The first is typical of silver nanoparticles of 20 nm, while the second is due to a weak clustering process of the nanoparticles.

The UV-Vis spectrum obtained from the colloidal solution-wine mixture (fig. 2a) shows two pronounced peaks of plasmon resonance to 439 nm and 561 nm. The shift of the first peak is compatible with an increase of the size of the nanoparticles and of the corona, while the second pronounced peak indicates that the wine promotes nanoparticles clustering.

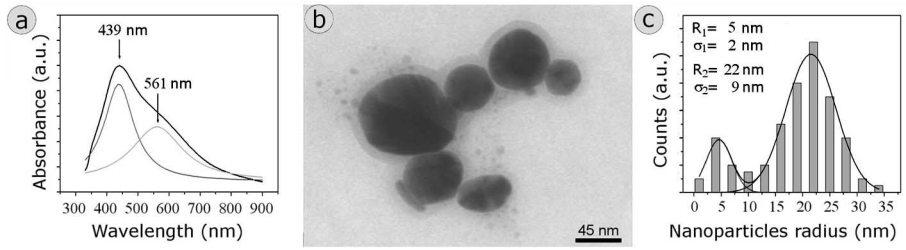

Fig. 2. – UV-Vis spectrum (a); transmission electron microscope image (b); nanoparticles size distribution (c) recorded from the mixture wine-Ag colloidal solution.

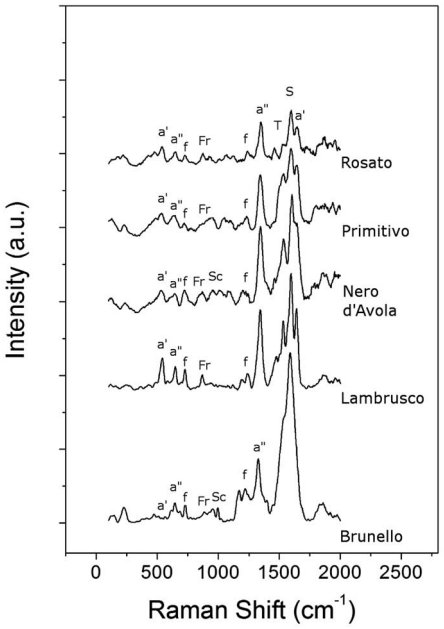

Fig. 3. – SERS spectra from different wine samples.

3˙2. *SERS measurements*. – The nanoparticles clustering determines the presence of the absorption band at 561 nm UV-Vis, also allows the SERS effect and the removal of the effects of fluorescence otherwise crucial in the Raman spectrum.

Figure 3 shows typical SERS spectra of some examined wine samples. The analysis of SERS spectra is not easy owing to large difference observed between the pure compounds reported in literature and the wine samples and to the number of different compounds present in each wine samples. In general, all the red wines examined show a similar spectrum below $1000\,\mathrm{cm}^{-1}$.

The main differences between all samples are found in the 1000–$2000\,\mathrm{cm}^{-1}$ region, where the bending (O–H) and stretching (C–O) motions appear, because of the different distribution of OH groups in the molecules presents in wines [18]. This points out the importance of the vibrational spectra in the identification of the constituents compounds and in the discrimination of the different wines.

However, on the basis of literature data we can attribute, reasonably, the observed peaks to anthocyanidin monoglyclosides and diglycosides, sulfite compounds, phenols, tetraterpenes, stilbenes, as summarized in table II.

The main differences between all samples in the 500 and $900\,\mathrm{cm}^{-1}$ spectral range strongly depends on the glycosylation pattern. Chemically anthocyanins are based on a C–15 skeleton with a chromane ring bearing a second aromatic ring B in position 2 and with one or more sugar molecules bonded at different hydroxylated positions of the basic structure; they are substituted glycosides of salts of phenyl-2-benzopyrilium (anthocyanidins). When the C–5 position is glycosylated the significant perturbations of spectral features between 640 and $750\,\mathrm{cm}^{-1}$ are visible, but they depend also on the nature of the individual sugar. Anthocyanidin monoglycosides exhibit a strong Raman signal close to $540\,\mathrm{cm}^{-1}$ while 3,5-diglycosides have the strongest feature in the lower frequency range

TABLE II. – *SERS modes assignment.*

Peak position, cm^{-1}	Assignments	Label
540	Anthocyanidin monoglycosides	a′
630	Anthocyanidin diglycosides	a″
723	phenols	f
870	fructose	Fr
980	sulfite compounds	Sc
1240	phenols	f
1350	Anthocyanidin diglycosides	a″
1512	Anthocyanidin diglycosides	a″
1530	tetraterpenes	T
1595	stilbenes	S
1645	Anthocyanidin monoglycosides	a′

close to $630\,cm^{-1}$. Additionally, both types of glycosides differ also in the relative intensity and in the shape of two lines located at 1645 and $1350\,cm^{-1}$ [19]. It is reported the $980\,cm^{-1}$ band to S–O stretching mode of sulfite compounds [20]. From comparison of different wines, this band appears appreciably only in the samples of Brunello and Nero d'Avola. This result may mean a higher concentration of sulphites in these wines. The band at $1595\,cm^{-1}$ can be assigned to (C=C) of the phenyl groups of stilbenes compounds. trans-Stilbene and several cyclic derivatives with hindered free rotation around the C(vinyl) C(phenyl) single bond were studied by various spectroscopic techniques, in particular several authors show that phenyl vibration is found in the expected region at $1595\,cm^{-1}$, while the weak vinyl stretching band occur at $1618\,cm^{-1}$ [21, 22]. Terpenes occur in plants as minor components at the ppm level. Strong bands of terpenes are observed in the Raman spectrum within the 1500–1550 and 1100–$1200\,cm^{-1}$ ranges due to in-phase C=C (1) and C–C stretching (2) vibrations of the polyene chain. Additionally, in-plane rocking mode of CH_3 groups attached to the polyene chain and coupled with C–C bonds are seen as a peak of low intensity in the 1000–$1020\,cm^{-1}$ region [23].

4. – Conclusions

We have reported, for the first time, the surface-enhanced Raman scattering (SERS) spectra of different kinds of red wine from grapes using erytrithol-aggregated fructose-reduced silver (Ag) colloids. The technique provided a substantial spectral enhancement and therefore good-quality spectra of all red-wine samples. The SERS profiles, through a precise band assignment allowed the fingerprint determination of the samples. The differences in the SERS profiles highlight those compositional differences that determine the organoleptic features. The main differences among the various samples can be attributed to the anthocyanidin and terpenes compounds, responsible for the staining and the scent of different wines. The suggested analysis can be applied to distinguish the polyphenolic composition of wines in order to identify, for example, the wine origin or to preserve quality wines from counterfeiting. The Raman spectroscopy come into sight as a feasible method for such purposes and alternative to the existing laboratory methods. In fact this method allows the evaluation of the sample composition in a few seconds and it produces a spectral pattern unique to each element, thus supplying precise information about the molecular composition of the sample.

REFERENCES

[1] Filippo E., Serra A., Manno D., *Colloids and Surfaces A: Physicochem. Eng. Aspects*, **348** (2009) 205.
[2] Csaki A., Berg S., Jahr N., Leitere C., Schneider T., Steinbruck A., Zopf D. and Fritz W., *Plasmonic nanoparticles - noble material for sensoric applications*, in *Gold Nanoparticles: Properties, Characterization and Fabrication* (Nova Science Publisher) 2010, pp. 245-261.
[3] Serra A., Manno D., Filippo E., Buccolieri A., Urso E., Rizzello A. and Maffia M., *Sensors Actuators B: Chemical*, **156** (2011) 479.
[4] Ditlbacher H., Krenn J. R., Schider G., Leitner A. and Aussenegg F. R., *Appl. Phys. Lett.*, **81** (2002) 1762.
[5] Rosenberg S., Shenoi R. V., Vandervelde T. E., Krishna S. and Painter O., *Appl. Phys. Lett*, **95** (2009) 161101.
[6] Atwater H. A. and Polman A. B., *Nat. Mater.*, **9** (2006) 205.
[7] Lassiter J. B., Sobhani H., Fan J. A. and Capasso F., *Nano Lett.*, **8** (2010) 3184.
[8] Langhammer C., Schwind M., Kasemo B. and Zoric I., *Nano Lett.*, **8** (2008) 1461.
[9] Stewart M. E., Anderton C. R., Thompson L. B., Maria J., Gray S. K., Rogers J. A. and Nuzzo R. G., *Chem. Rev.*, **108** (2008) 494.
[10] Choi Y., Choi D. and Lee L. P., *Adv. Mater*, **22** (2010) 1754.
[11] Homola J., *Chem. Rev.*, **108** (2008) 462.
[12] McQuillan A. J., *Notes Rec. R. Soc.*, **63** (2009) 783.
[13] Moskovits M., *Rev. Mod. Phys.*, **57** (1985) 12; **69** (999) 1666.
[14] Zhang X., Young M. A., Lyandres O. and Van Duyne R. P., *J. Am. Chem. Soc.*, **127** (2005) 4484.
[15] Hering K., *Bioanal. Chem.*, **390** (2008) 113.
[16] Grubisha D. S., Lipert R. J., Park H. Y., Driskell J. and Porter M. D., *Anal. Chem.*, **75** (2003) 5936.
[17] Patel K., Kapoor S., Dave D. P. and Mukherjee T., *J. Chem. Sci.*, **117** (2005) 53.
[18] Schulz H. and Baranska M., *Vibr. Spectr.*, **43** (2007) 13.
[19] Picard A., Daniel I., Montagnac G. and Oger P., *Extremophiles*, **11** (2007) 445.
[20] Ball S. and Milne J., *Can. J. Chem.*, **73** (1995) 716.
[21] Sanchez-Cortes S. and Garcia-Ramos J. V., *Spectr. Chim. Acta Part A*, **55** (1999) 2935.
[22] Billes F., Mohammed-Ziegler I., Mikosch H. and Tyihac E., *Spectr. Chim. Acta Part A*, **68** (2007) 669.
[23] Schulz H., Baranska M. and Baranski R., *Biopolymers*, **77** (2005) 358.